

# A Fully Coupled Poroelastic Reactive-Transport Model of Cartilage

Lihai Zhang\*, Bruce S. Gardiner\*, David W. Smith\*, Peter Pivonka\* and Alan Grodzinsky†

**Abstract:** Cartilage maintains its integrity in a hostile mechanical environment. This task is made more difficult because cartilage has no blood supply, and so nutrients and growth factors need to be transported greater distances than normal to reach cells several millimetres from the cartilage surface. The chondrocytes embedded within the extracellular matrix (ECM) are essential for maintaining the mechanical integrity of the ECM, through a balance of degradation and synthesis of collagen and proteoglycans. A chondrocyte senses various chemical and mechanical signals in its local microenvironment, responding by appropriate adaption of the local ECM. Clearly a 'systems understanding' of cartilage behaviour is of critical importance in developing an integrated understanding of both normal and abnormal physiology of cartilage. In a series of papers, we have developed a reactive-transport poro-media model to investigate the coupled processes of growth factor transport, mechanical deformation and fluid flow, and in this paper, we extend the model to include biosynthesis and degradation of matrix molecules. The model is validated using three independent experimental data sets, it being found that a single set of parameters described the experimental results remarkably well. The model is then employed to make predictions about changes in proteoglycan content under a variety of conditions. This model may prove useful in predicting the behaviour of tissue engineering constructs, or predicting the outcome of repair processes in cartilage.

**Keyword:** IGF-I; glycosaminoglycan; mechan-

ical stimuli; transport, biosynthesis, degradation.

## 1 Introduction

Articular cartilage needs to maintain its integrity in a hostile mechanical environment. Injuries to cartilage (perhaps due to disease processes or traumatic impact loading) are a common source of chronic debilitation, and so increasing our understanding of the processes governing cartilage homeostasis are critical to an informed understanding of abnormal physiological processes. Current limitations in our understanding restrict our ability to interpret cartilage behaviours and develop strategies to repair damaged cartilage, or to engineer replacements. At least in part this is due to the complexity of the system. For example, cartilage matrix biosynthesis is known to be controlled by both the chemical and mechanical microenvironment of the chondrocytes. The transport of nutrients to chondrocytes in cartilage (which is part of the chemical environment) and the transport of newly synthesized matrix components, are also coupled with the mechanical environment, both directly through advective transport, and indirectly through changes in the matrix physical properties due to changes in biosynthesis. The system is further complicated by binding proteins embedded in the cartilage matrix, cell surface receptors, and the complexities of intracellular signaling pathways. The list of possible components and processes is daunting. There is a clear need for a model to integrate current and future experimental data about this complex system, and to explore the range of potential states of the system with the goal of identifying optimal strategies for maintaining healthy cartilage or growing new cartilage for implantation. To this end, we have been systematically developing a fully coupled model of cartilage biosynthesis.

\* Department of Civil and Environmental Engineering, The University of Melbourne, VIC 3010, Australia

† Center for Biomedical Engineering, Departments of Electrical Engineering and Computer Science, Biological Engineering and Mechanical Engineering, Massachusetts Institute of Technology, Cambridge, Massachusetts, USA

This model includes: IGF-I reactive-advective-diffusive transport, competitive binding of IGF-I to two functional groups of IGF-BPs, binding to a single group of cell surface receptors, receptor-IGF-I endocytosis, receptor recycling, IGF-I induced proteoglycan (aggrecan) biosynthesis, interstitial fluid flow-induced proteoglycan biosynthesis, basal proteoglycan biosynthesis, and proteoglycan hindered reactive-advective-diffusional transport and degradation. The reactive-transport model described is formulated within a fully coupled poro-elastic model of cartilage that includes compression-tension nonlinearity.

Approximately 25% of the wet weight of articular cartilage is composed of proteoglycans. Aggrecan monomers are the predominant proteoglycan constituents in the ECM; they are relatively large molecules ( $3.5 \times 10^6$  Da), with a central protein core containing up to  $\sim 100$  chondroitin sulfate GAG chains [1]. These negatively charged GAGs generate an osmotic (or disjoining) swelling pressure through the presence of counterions, and this GAG concentration contributes substantially to the compressive stiffness of cartilage [2].

Most proteoglycans (around 60–80%) within the interterritorial matrix are believed to be in stable forms (i.e., effectively immobilized within the ECM). Newly synthesized aggrecan monomers, continually secreted by the chondrocytes, are mobile until the majority become bound to hyaluronan in the form of supramolecular aggregates; other newly synthesized aggrecan monomers may be lost from the tissue by diffusion. Finally, under normal turnover conditions, a small population of newly synthesized and/or pre-existing aggrecan are degraded, predominantly by one of the aggrecanases [1]. These aggrecan molecules are soluble and mobile in interstitial fluid, and may be transported through the ECM [3-5]. Indeed, the newly synthesized aggrecans need to be transported away from chondrocytes after secretion and ultimately incorporated into the tissue matrix, while degraded aggrecans may find their way out of the cartilage ECM and into the synovial fluid.

DiMicco et al [6] theoretically studied the steady-state metabolism and transport of the cartilage matrix components using a continuum model.

Most importantly, they modeled the matrix molecules as three groups—soluble, bound and degraded components and investigated the synthesis, binding, and transport behaviour of each component, and their interactions. Klein et al [7] later extended this continuum model to understand the effects of membrane permeability and perfusion on proteoglycan accumulation in tissue engineered cartilage. However, as cartilage tissue survives in an extremely hostile mechanical environment, a plausible model should be able to describe both the mechanical behavior of cartilage and the important transport mechanisms (e.g., for IGFs and matrix components (e.g. aggrecan)) [8, 9]. Moreover, the contribution of biochemical stimuli (e.g., growth factors) and mechanical stimuli (e.g., interstitial fluid flow) to the biosynthesis of cartilage needs to be included in the model.

It is known that tissue growth factors (e.g., IGFs) are important stimuli for cartilage extracellular matrix (ECM) synthesis and assembly [10]. However, a great deal of evidence suggests that physiological relevant dynamic loading alone can also stimulate cartilage synthesis [11]. For example, recent in-vivo studies using Magnetic Resonance Imaging technology reported positive effects of moderate exercise on improving GAG content in human knee cartilage [12]. However in a carefully planned set of experiments Buschmann et al [13] clearly indicated the role of interstitial fluid flow in the stimulation of proteoglycan production in calf cartilage explants, and presented evidence supporting the hypothesis that dynamic loading induced biosynthesis depends on a certain threshold of interstitial fluid velocity. In addition, the mechanical stimulation was shown to be dependent on the frequency of applied load or applied strain, as well as the duration of the mechanical stimuli.

The study of matrix protein metabolism in tissue engineered cartilage constructs by Davisson et al., 2002..[14] found that static compression at 50% strain diminished GAG synthesis by 57%. In contrast, a dynamic loading compression at 0.1 Hz increased the GAG production by 179%. Buschman et al [13] also observed a uniform ag-

greacan synthesis in cartilage explants undergoing unconfined cyclic compression at intermediate frequency of 0.01 Hz, and most importantly, the aggrecan biosynthesis was only seen in peripheral regions at a higher frequency of 0.1 Hz.

Interstitial fluid flow not only induces ECM biosynthesis, but also can enhance solute transport within the cartilage tissue [11]. For small solutes with large diffusion coefficient in range of  $2\text{-}6 \times 10^{-6} \text{ cm}^2/\text{s}$ , fluid advective transport does not significantly affect solute transport. However, fluid movement may noticeably affect the transport of large solutes with small diffusion coefficient (e.g.,  $2 \times 10^{-7} \text{ cm}^2/\text{s}$ ) [15] (i.e. for these molecules the Peclet number is much higher). Indeed this was shown to be the case for IGF molecules [16].

Newly synthesized mobile aggrecans are very large molecules with very small diffusion coefficients in the range of  $10^{-10} - 10^{-9} \text{ cm}^2/\text{s}$  [17], and so dynamic loading is expected to significantly influence their transport. However, as cartilage ECM itself contains many large immobilized or bound molecules, this may decrease the mobility of macromolecules and so limit their transport. For this reason we include hindered advective transport in the governing transport equations.

Obviously, cartilage is a complex system involving different transport characteristics, and a clear systems level understanding is required. The aim of this study is to develop an integrated computational model to investigate the coupled processes of growth factor and matrix macromolecule transport, as well as IGF-I and mechanical stimuli mediated aggrecan biosynthesis behavior within the cartilage. The model builds upon our previous publications on fully-coupled mechanical and solute transport processes, growth factors competitive binding to IGFBs and cell surface receptors [16, 18-20]. In this paper, we extend the model to include proteoglycan formation and degradation.

The paper first describes the model within the framework of porous media theory, which includes our previous reactive-transport modeling of IGF. The new model, which includes proteoglycan formation and degradation, is based on the

findings of three independent experimental studies [13, 21, 22]. Our aim is to harmonise these experimental findings, in the sense of obtaining a unique set of model parameters that explain the observed system behavior in each of the experimental systems. After validating the model, it is used in a predictive capacity to demonstrate the expected response of cartilage to loading and IGF stimulation. The fundamental objective of this study is to construct a quantitative model to enhance our understanding of cartilage homeostasis, both in-vivo and in-vitro.

## 2 Model description

While the detailed mechanisms of cartilage biosynthesis and degradation behavior are far from clear at the present time, there is experimental evidence indicating that growth factors such as IGF-I and the mechanical loading are key factors that can regulate matrix biosynthesis. To calculate the microenvironment that informs these response mechanisms, we make the following assumptions:

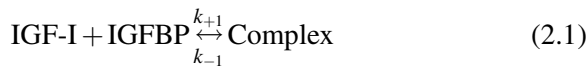
- The IGF binding proteins (IGFBPs) and chondrocytes are effectively immobilized in the tissue ECM. IGFs may bind to cell surface receptors (R1) and IGFBPs simultaneously.
- Forming the IGF-I/R1 complex (R1I) initiates an intercellular signaling cascade which ultimately leads to the production of cartilage ECM constituents (e.g. aggrecan and its constituent GAG chains). IGF-I may also be internalized during the process [23].
- The major function of IGFBPs is to sequester IGFs, but it is the ‘free’ IGF that is the functionally active form. IGFBPs can be classified into two functional groupings [19]. The first grouping has approximately similar binding affinity to both IGF-I and -II (i.e. IGFBPs 1-5), whereas the second group has significantly higher binding preference for IGF-II compared to IGF-I (i.e. IGFBP-6).
- As experiments have demonstrated that chondrocytes synthesize little or no IGF-I

under explant culture conditions [10], it is reasonable to assume the majority of IGF-I in cartilage is supplied from synovial fluid.

- In the framework of porous media theory, articular cartilage is modeled as a three phase mixture, namely, a solute phase that includes mobile IGF-I and aggrecan molecules, a fluid phase representing interstitial fluid, and a solid phase representing immobilized ECM.

### 2.1 IGF-I transport

The reversible reaction involving IGF-I, receptors and IGFBPs can be described by:



Using the law of mass action [20], equations (2.1) and (2.2) can be included in the reactive-transport equations for IGF-I and IGFBPs as follows,

$$\frac{d\bar{c}_I^f}{dt} = -\nabla \cdot \left( -D_I \nabla \bar{c}_I^f + v^f \bar{c}_I^f \right) - k_{+1} \bar{c}_I^f \bar{c}_{BP} + k_{-1} \bar{c}_I^b - k_{+2} \bar{c}_I^f \bar{c}_{R1} + k_{-2} \bar{c}_{R1I} \quad (2.3a)$$

$$\frac{d\bar{c}_I^b}{dt} = -\nabla \cdot \left( v^s \bar{c}_I^b \right) + k_{+1} \bar{c}_I^f \bar{c}_{BP} - k_{-1} \bar{c}_I^b \quad (2.3b)$$

$$\frac{d\bar{c}_{BP}}{dt} = -k_{+1} \bar{c}_I^f \bar{c}_{BP} + k_{-1} \bar{c}_I^b \quad (2.3c)$$

$$\frac{d\bar{c}_{R1}}{dt} = -k_{+2} \bar{c}_I^f \bar{c}_{R1} + (k_{-2} + k_0) \bar{c}_{R1I} \quad (2.3d)$$

$$\frac{d\bar{c}_{R1I}}{dt} = k_{+2} \bar{c}_I^f \bar{c}_{R1} - (k_{-2} + k_0) \bar{c}_{R1I} \quad (2.3e)$$

where  $\bar{c}_I^f$ ,  $\bar{c}_{BP}$ ,  $\bar{c}_I^b$ ,  $\bar{c}_{R1}$  and  $\bar{c}_{R1I}$  are volume based IGF-I, IGFBP, IGF-I/IGFBP complex, receptor and IGF-I/receptor complex concentrations respectively.  $D_I$  is the diffusion coefficient of IGF-I,  $k_{+1}$ ,  $k_{-1}$ ,  $k_{+2}$ ,  $k_{-2}$  and  $k_0$  the reaction rate constants that have been estimated from published experimental studies (see Table 1), while  $v^f$  and  $v^s$  are the fluid and solid phase velocities respectively.

### 2.2 Aggrecan transport

After being secreted, newly synthesized aggrecan molecules are initially mobile and move into the surrounding matrix, where they become bound to hyaluronan as proteoglycan aggregates and so become much less mobile. (In this paper, we assume that they effectively become immobile when incorporated into the ECM as aggregates). Similarly, other secreted matrix molecules can become assembled within the ECM; however, we focus in this study on aggrecan. Aggrecan (and other ECM macromolecules) can eventually be degraded; when degraded, they become mobile again, and are potentially released from matrix [6] finding their way into the synovial fluid. The total matrix aggrecan concentration in cartilage ( $\bar{c}_a$ ) is the sum of chondrocyte-derived mobile component transported in fluid phase ( $\bar{c}_a^f$ ); ‘immobilized’ proteoglycan component effectively ‘bound’ within ECM ( $\bar{c}_a^b$ ), and finally the mobile component degraded from the ECM structure ( $\bar{c}_a^d$ ) (which may escape from the cartilage altogether). So the total aggrecan concentration is given by,

$$\bar{c}_a = \bar{c}_a^f + \bar{c}_a^b + \bar{c}_a^d \quad (2.4)$$

The transport equation of each component is represented as:

$$\frac{d\bar{c}_a^f}{dt} + \nabla \cdot \left( -K_d D_a \nabla \bar{c}_a^f + K_a v^f \bar{c}_a^f \right) = s_p - s_b \bar{c}_a^f \quad (2.5)$$

$$\frac{d\bar{c}_a^b}{dt} = s_b \bar{c}_a^f - s_d \bar{c}_a^b \quad (2.6)$$

$$\frac{d\bar{c}_a^d}{dt} + \nabla \cdot \left( -K_d D_a \nabla \bar{c}_a^d + K_a v^f \bar{c}_a^d \right) = s_d \bar{c}_a^b \quad (2.7)$$

where  $D_a$  is diffusion coefficient of free aggrecan.  $K_d$  is a dimensionless tortuosity coefficient, and  $K_a$  a dimensionless hindrance coefficient. The values of  $K_d$  and  $K_a$  depend on molecular size and shape of the molecule being transported through the ECM.  $s_b$  and  $s_d$  are aggrecan binding and degradation rate respectively, which are obtained from experimental studies [6, 7].

Table 1: Material parameters used throughout this study.

Parameter	Value	Ref
Radius of cartilage disc ( $r_0$ )	1.5 mm	[21]
Hydraulic permeability ( $\kappa_r$ )	$2 \times 10^{-15} \text{ m}^4/\text{Ns}$	[33]
Diffusion coefficient of IGF-I ( $D_I$ )	$(3-6) \times 10^{-12} \text{ m}^2/\text{s}$	[34]
Diffusion coefficient of aggrecan	$10^{-9}-10^{-10} \text{ m}^2/\text{s}$	[6]
Fluid phase volumetric fraction ( $\phi^f$ )	0.8	[21, 33]
Dissociation constant for IGF-I and IGFBPs 1-5	4.8 nM	[19]
IGFBPs concentration ( $c_{BP0}$ )	30-150 nM	[35]
Associate rate constant for IGF-I and receptors ( $k_{+2}$ )	$(0.2 - 0.5)k_{+1}$	[36]
Dissociate rate constant for IGF-I and receptors ( $k_{-2}$ )	$k_{-2}/k_{+2} = (0.5 - 2.5) \times 10^{-6} \text{ M/m}^3$	[36]
Receptor internalization rate ( $k_0$ )	$(0.5 - 3)k_{-2}$	[36]
Aggrecan binding rate ( $s_b$ )	$1.2 \times 10^{-5} \text{ s}^{-1}$	[7]
Aggrecan degradation rate ( $s_d$ )	$3.7 \times 10^{-7} \text{ s}^{-1}$	[7]
Basal synthesis rate of bovine cartilage ( $s_{p0}$ )	$1.9 \times 10^{-8} \text{ g/cm}^3 \cdot \text{s}$	[6]
Total aggrecan concentration in normal bovine cartilage ( $\bar{c}_{a0}$ )	(10-50) mg/ml	[30, 31]
Maximum cartilage aggrecan concentration ( $\bar{c}_{a\text{max}}$ )	5% - 5.7% wet weight	[26]
Total receptor concentration ( $\bar{c}_{RT}$ )	0.6 nM	[36]
Tensile aggregate modulus ( $H_{+A}$ )	13.2 MPa	[27]
Compressive Poission ratio ( $\nu$ )	$\leq 0.045$	[27]

### 2.3 Aggrecan biosynthesis

Consistent with experimental observations, the aggrecan production rate  $s_p$  is here taken to be the sum of the basal production rate  $s_{p0}$  [7], IGF-I mediated production rate  $s_{pI}$ , and mechanical stimuli induced production rate  $s_{pm}$ . That is

$$s_p = s_{p0} + s_{pI} + s_{pm} \quad (2.8)$$

The production rates  $s_{pI}$  and  $s_{pm}$  can be defined by so-called ‘‘Hill functions’’, which are commonly employed in the physiology [24]. Our previous study [20] suggested  $s_{pI}$  depends on the number of IGF-I ligands bound to chondrocyte receptors (i.e.  $\bar{c}_{RII}$ ). It is also limited by the maximum aggrecan concentration (i.e.  $\bar{c}_{a\text{max}}$ ) possible in the cartilage tissue [25]. The cellular response to mechanical stimuli has been reported to exhibit a threshold behaviour, with production triggered when the interstitial fluid Darcy’s velocity ( $v_d$ ) reaching a certain threshold ( $v_0$ ) [13]. No apparent dose dependence of aggrecan production on

fluid velocity was observed experimentally [13]. Based on these observations, the aggrecan production rate is here taken to be,

Chemical stimuli

$$s_{pI} = \left( \frac{\beta \bar{c}_{RII}^n}{K^n + \bar{c}_{RII}^n} \right) \left( 1 - \frac{\bar{c}_a^f + \bar{c}_a^b}{\bar{c}_{a\text{max}}} \right) \quad (2.9)$$

Mechanical stimuli

$$s_{pm} = \begin{cases} \lambda \left( 1 - \frac{\bar{c}_a^f + \bar{c}_a^b}{\bar{c}_{a\text{max}}} \right), & (|v_d| \geq v_0) \\ 0, & (|v_d| < v_0) \end{cases} \quad (2.10)$$

$$v_d = \phi^f (v^f - v^s) = -\kappa \nabla p \quad (2.11)$$

where parameter  $K$  is the ‘activation coefficient’,  $n$  defines the steepness of the Hill function,  $\beta$  is the IGF-I mediated maximum production rate,  $\lambda$  mechanical mediated production rate,  $\phi^f$  volume fraction of fluid phase,  $v_d$  the Darcy velocity,  $\kappa$  the permeability tensor,  $p$  the interstitial fluid

pressure, and  $\bar{c}_{a\max}$  the maximum aggrecan concentration possible in the tissue [26]. The mechanical quantities, such as  $v^f$ ,  $v^s$  and  $p$  can be estimated using methods as described in our previous published studies and so are not elaborated further here [16, 18].

### 3 Unconfined dynamic compression

Consistent with experimental protocols employed for studying the biosynthetic response of cartilage explants to IGF-I or mechanical stimuli [13, 21], the model geometry considered here describes unconfined compression of a tissue explant. Consequently the governing equations are presented in cylindrical coordinates, viz,

- (i) Equations describing IGF-I transport and interaction with IGF-BPs and receptors

$$\begin{aligned} & \phi^f \frac{\partial c_I^f}{\partial t} - \phi^f D_I \left( \frac{\partial^2 c_I^f}{\partial r^2} + \frac{1}{r} \frac{\partial c_I^f}{\partial r} \right) \\ & + \left( \phi^f v_r - \kappa_r \frac{\partial p}{\partial r} \right) \frac{\partial c_I^f}{\partial r} \\ = & -k_{+1} \phi^f (1 - \phi^f) c_I^f c_{BP} + k_{-1} (1 - \phi^f) c_I^b \\ & - k_{+2} \phi^f (1 - \phi^f) c_I^f c_{R1I} + k_{-2} (1 - \phi^f) c_{R1I} \end{aligned} \quad (3.1)$$

$$\frac{\partial c_I^b}{\partial t} + v_r \frac{\partial c_I^b}{\partial r} = k_{+1} \phi^f c_I^f c_{BP} - k_{-1} c_I^b \quad (3.2)$$

$$\frac{dc_{BP}}{dt} = -k_{+1} \phi^f c_I^f c_{BP} + k_{-1} c_I^b \quad (3.3)$$

$$\frac{dc_{R1I}}{dt} = -k_{+2} \phi^f c_I^f c_{R1I} + (k_{-2} + k_0) c_{R1I} \quad (3.4)$$

$$\frac{dc_{R1I}}{dt} = k_{+2} \phi^f c_I^f c_{R1I} - (k_{-2} + k_0) c_{R1I} \quad (3.5)$$

- (ii) Equations describing aggrecan molecule transport, production, binding and degrada-

tion

$$\begin{aligned} & \phi^f \frac{\partial c_a^f}{\partial t} - \phi^f K_d D_a \left( \frac{\partial^2 c_a^f}{\partial r^2} + \frac{1}{r} \frac{\partial c_a^f}{\partial r} \right) \\ & + K_a \left( \phi^f v_r - \kappa_r \frac{\partial p}{\partial r} \right) \frac{\partial c_a^f}{\partial r} \\ = & \left( s_{p0} + \frac{\beta c_{R1I}^n}{K^n + c_{R1I}^n} + \lambda \right) \\ & \left[ 1 - \frac{\phi^f c_a^f + (1 - \phi^f) c_a^b}{c_{a\max}} \right] - s_b \phi^f c_a^f \end{aligned} \quad (3.6)$$

$$(1 - \phi^f) \frac{\partial c_a^b}{\partial t} = s_b \phi^f c_a^f - s_d (1 - \phi^f) c_a^b \quad (3.7)$$

$$\begin{aligned} & \phi^f \frac{\partial c_a^d}{\partial t} - \phi^f K_d D_a \left( \frac{\partial^2 c_a^d}{\partial r^2} + \frac{1}{r} \frac{\partial c_a^d}{\partial r} \right) \\ & + K_a \left( \phi^f v_r - \kappa_r \frac{\partial p}{\partial r} \right) \frac{\partial c_a^d}{\partial r} = s_d (1 - \phi^f) c_a^b \end{aligned} \quad (3.8)$$

- (iii) Equations describing the mechanical behavior of cartilage

$$\frac{v_r}{r} + \frac{\partial v_r}{\partial r} + \frac{\partial \varepsilon_z}{\partial t} - \kappa_r \left( \frac{\partial^2 p}{\partial r^2} + \frac{1}{r} \frac{\partial p}{\partial r} \right) = 0 \quad (3.9)$$

$$-\frac{\partial p}{\partial r} + H_{+A} \left( -\frac{u_r}{r^2} + \frac{1}{r} \frac{\partial u_r}{\partial r} + \frac{\partial^2 u_r}{\partial r^2} \right) = 0 \quad (3.10)$$

where  $\varepsilon_z = (\partial u_z / \partial z)$  is the applied time-dependent axial strain and  $v_r = (\partial u_r / \partial t)$  is the radial component of the solid phase velocity. It has been found that cartilage has different mechanical properties under tension and compression, and so this is included in the model [27]. Equation (3.10) is obtained from the Conewise Linear Elasticity model with cubic symmetry.  $H_{+A}$  is the tensile aggregate modulus [27].

The applied strain is in the axial direction and is a sinusoid, i.e.

$$\varepsilon_z = -\frac{\varepsilon_0}{2} [1 - \cos(2\pi ft)] \quad (3.11)$$

where  $\varepsilon_0$  is the peak-to-peak strain amplitude and  $f$  is the loading frequency.

### 3.1 Boundary and initial conditions

To close the set of partial differential equations described above, boundary conditions and initial conditions are required. At the outer edge of the cartilage (i.e.  $r = r_0$ ) the following boundary conditions apply:

- (i) For fluid pressure and solid phase displacement:

$$p(r_0, t) = 0, \quad \frac{\partial u_r(r_0, t)}{\partial r} = -\frac{\nu}{1-\nu} \left[ \frac{u_r(r_0, t)}{r_0} + \varepsilon_z \right] \quad (3.12a)$$

- (ii) For IGF-I:

$$c_I^f(r_0, t) = c_{I0} \quad (3.12b)$$

- (iii) For aggrecan:

$$c_a^f(r_0, t) = 0, \quad c_a^d(r_0, t) = 0 \quad (3.12c)$$

At the centre of the cartilage (i.e.  $r = 0$ ), the following boundary conditions apply:

- (i) Fluid pressure and solid phase displacement:

$$u_r(0, t) = 0, \quad \frac{\partial p(0, t)}{\partial r} = 0 \quad (3.13a)$$

- (ii) For IGF-I:

$$\frac{\partial c_I^f(0, t)}{\partial r} = 0, \quad \frac{\partial c_I^b(0, t)}{\partial r} = 0 \quad (3.13b)$$

- (iii) For aggrecan:

$$\frac{\partial c_a^f(0, t)}{\partial r} = 0, \quad \frac{\partial c_a^d(0, t)}{\partial r} = 0 \quad (3.13c)$$

where  $c_{I0}$  is the bath solute concentration, and  $\nu$  is the compressive Poisson's ratio.

For the simplicity, the initial conditions are assumed to be constant throughout the tissue.

- (i) Fluid pressure and solid phase displacement:

$$u_r(r, 0) = 0, \quad p(r, 0) = 0 \quad (3.14a)$$

- (ii) For IGF-I:

$$c_I^f(r, 0) = 0, \quad c_I^b(r, 0) = c_{b0} \quad (3.14b)$$

- (iii) For aggrecan:

$$\bar{c}_a^f(r, 0) = 0, \quad \bar{c}_a^b(r, 0) = \bar{c}_{a0}, \quad \bar{c}_a^d(r, 0) = 0 \quad (3.14c)$$

where  $c_{b0}$  is initial IGFBP concentration, and  $\bar{c}_{a0}$  the volume-based initial total aggrecan concentration. The model was solved numerically, using the commercial finite element software package COMSOL [28]. The applied strain deformation is represented through time discretization. At each time step, the mechanical quantities, like solid phase displacement and velocity are calculated, and these quantities are then used to describe the transport behavior of IGF-I and mobile aggrecan molecules. A one-dimensional domain in the radial direction represented by 150 quadratic Galerkin elements was used for all calculations, and relatively small tolerances (relative tolerance  $10^{-8}$ , absolute  $10^{-9}$ ) were employed for all calculations. The FEM discretization of the time-dependent PDE problem is solved using an implicit solver of COMSOL.

## 4 Model validation

### 4.1 Parameter estimation for aggrecan production

Most of the transport and mechanical quantities are relatively well characterised based on previous studies. Table 1 lists the range of parameters used in this study, which are based on the previous estimates of these parameters.

In this study, we wish to extend our model to include the behaviour of aggrecan molecules and their associated GAG chains. This presents a number of challenges in estimating suitable model parameters. It is known that the diffusivity of mobile aggrecan is in the range of  $10^{-9}$  to  $10^{-10}$  cm<sup>2</sup>/s [6], however there is no information on aggrecans for the estimation of parameters representing hindered transport through ECM. Due to the unavailability of experimental information,  $K_a$  is first estimated from a study by Edwards et al [29] on hindered transport of macromolecules. The influence of this parameter on matrix macromolecule transport is further investigated by means of a parametric study described later in this paper.

Further challenges present themselves. Matrix formation and degradation are complex processes, and there is no absolute quantitative measurement of these rates in cartilage for any species to date. However, there have been numerous attempts to quantify aggrecan turnover. Some relevant information required for the model estimates can be obtained from the study of DiMicco et al [6] on tissue-engineered cartilage. They estimated the formation rate  $s_b$  from the half-time (4-24 hours) of the conversion of new synthesized low affinity aggrecan to high affinity aggrecan suitable for attachment to hyaluronan. The degradation rate of aggrecan  $s_d$  was calculated from the half-life (21 days) for the turnover in normal bovine cartilage explants. However, it is important to note that the values of  $s_b$  and  $s_d$  will undoubtedly vary from in-vitro to in-vivo and from species to species, as well as the stage of development of the individual animal. Thus, the parameter values of  $s_b$  and  $s_d$  adopted in this study based on the work of DiMicco can only be treated as a first estimate.

The greatest parameter uncertainty relates to aggrecan formation. However there are three independent studies on aggrecan synthesis performed on one to two week old calf cartilage explants, and we base our model developments on these studies [13, 21, 22]. Because these three studies were all done using bovine cartilage explants at the same stage of development, our challenge here is to find a single set of parameters that are

consistent with the aggrecan biosynthesis behaviour observed in all three independent experimental studies [13, 21, 22]. Parameters in Equations (2.9) and (2.10) related to aggrecan synthesis that need to be estimated include the coefficient  $n$ , the activation coefficient  $K$ , the IGF-I mediated maximum production rate  $\beta$ , and mechanical stimuli mediated production rate  $\lambda$ , as well as estimating the initial aggrecan concentration  $\bar{c}_{a0}$ . A major outcome of this paper is achieving this goal.

#### 4.2 Estimating aggrecan production in bovine cartilage explants

In the three independent experimental studies on aggrecan production [13, 21, 22], cylindrical cartilage explants (3mm in diameter and 1mm thick) from the femoropatellar groove of 1- to 2- week-old calves were tested. Buschmann et al. (1999) [13] studied the spatially distribution of biosynthesis in the cartilage explants in response to cyclic mechanical loading at frequencies of 0.01 – 0.1 Hz at displacement of amplitude of 50  $\mu$ m for 23 hours. The rate of aggrecan synthesis was assessed by measuring the <sup>35</sup>S-sulfate incorporation during the last 8 hours. Later Bonassar et al. (2000) [21] and Jin et al.(2003) [22] investigated the aggrecan synthesis when cartilage explants were exposed to a range of IGF-I concentrations under conditions of free diffusion. The <sup>35</sup>S-sulfate incorporation was also used to assess the effect of IGF-I on aggrecan synthesis.

Buschmann et al [13] reported that there is a correlation between dynamic loads induced local interstitial fluid velocities and matrix synthesis in cartilage. Buschmann et al. postulated that the stimulatory effect occurs in the regions where fluid velocity exceeds a certain threshold velocity, that is,  $v_0 = 0.25 \mu$ m/s [13]. However, one cannot discount the possibility that cell deformation is also important. Hence in Figure 1a-c show typical variation in Darcy's velocity profile through a single loading cycle under various loading conditions and in Figure 2 we show the radial strain profiles in a cartilage disk under similar dynamic loading. The numerical results in Figure 1 and Figure 2 do not support the hypothesis that increasing strain levels in solid matrix stimulate ag-

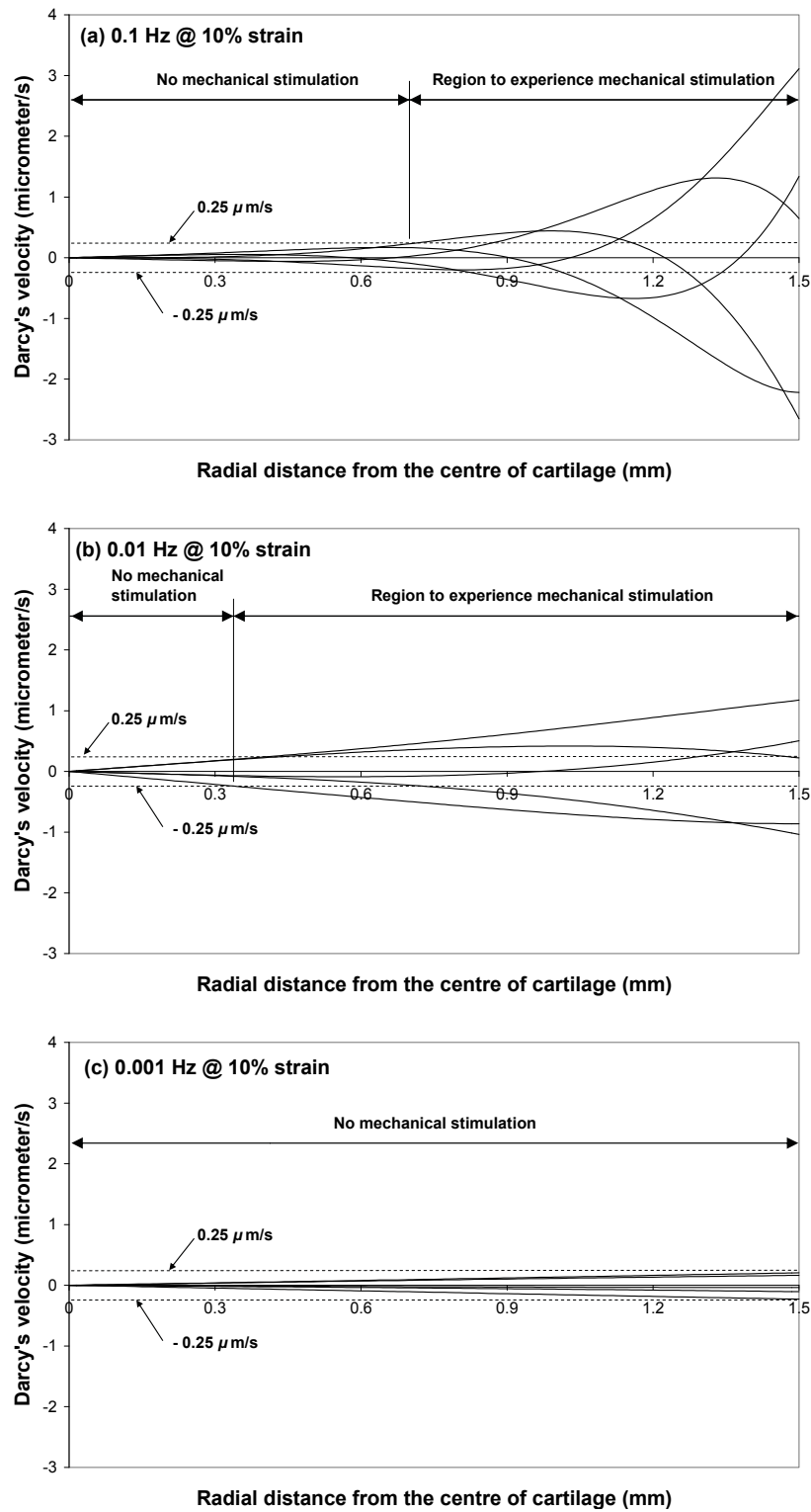


Figure 1: Darcy's velocity as a function of radial distance from centre of the cartilage for a number of time steps throughout a single loading cycle. (a) 0.1 Hz @ 10% strain, (b) 0.01 Hz @ 10% strain, (c) 0.001 Hz @ 10% strain. The aggrecan synthesis is stimulated when Darcy's velocity  $\geq v_0$  (i.e.  $0.25 \mu\text{m/s}$  [13]).

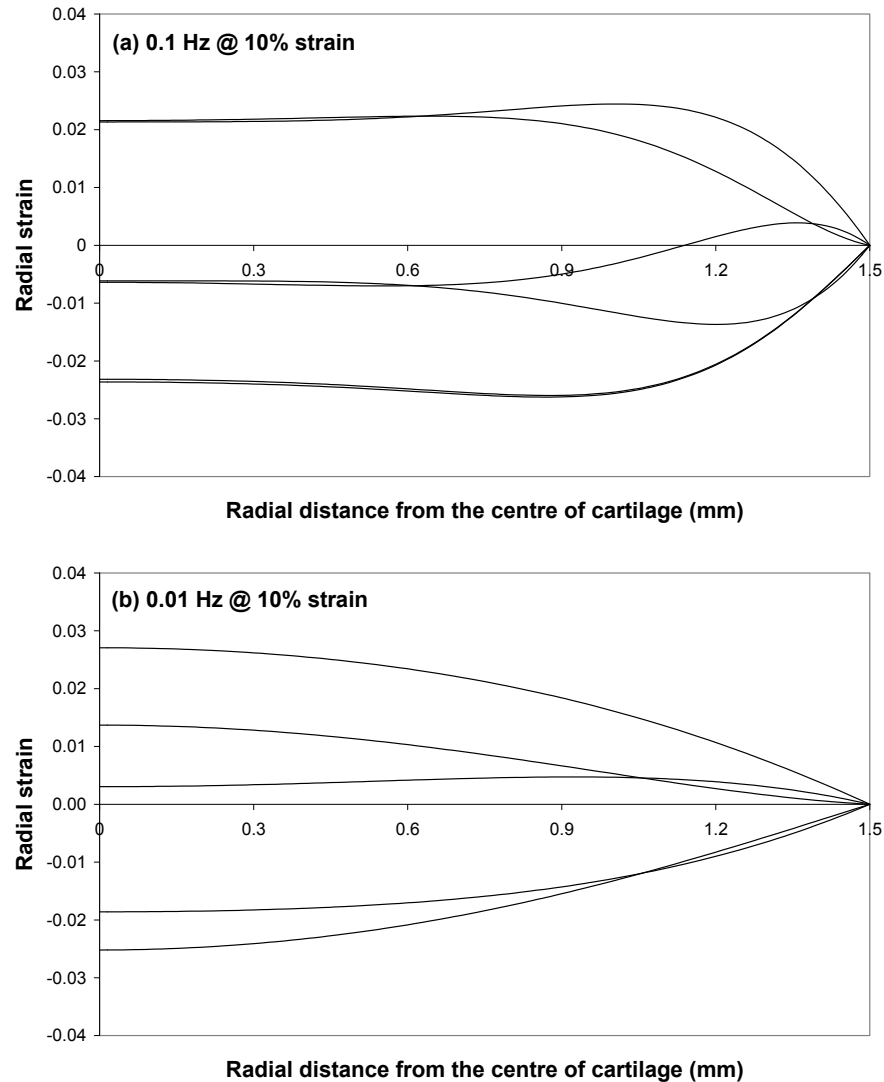


Figure 2: Radial strain as a function of radial distance from centre of the cartilage for a number of time steps throughout a single loading cycle. (a) 0.1 Hz@10% strain, (b) 0.01 Hz@10% strain.

grecan synthesis as strain profiles are predicted to decrease toward peripheral regions where matrix synthesis increases (Buschmann et al [13]). Hence, the numerical results of Darcy velocity profiles are employed to predict the aggrecan production at a first estimate.

We can see that numerical results based on Equations (2.10) and (2.11) fit well with the experimental data at the frequencies of 0.01 Hz (Figure 3a) and 0.1 Hz (Figure 3b) respectively when mechanical stimuli mediated production rate  $\lambda \approx 1 \times 10^{-5}$  mg/ml·s and  $\bar{c}_{a0} \approx 16$  mg/ml. It can be seen from Figure 3 that mechanical loading

stimulates aggrecan biosynthesis in a frequency and spatially dependent manner. Although a loading regime of high frequency 0.1 Hz results in the greatest fluid velocity, the mechanical stimulation is localized to the periphery domain. For the intermediate frequency of 0.01 Hz, the region experiencing mechanical stimulation extends into the inner region of the domain, whereas a low frequency at 0.001 Hz there was no stimulatory effect. The current study underlines the importance of the optimal selection of dynamic loading regimes to stimulate matrix synthesis in cartilage, which has obvious application in tissue engineering, and possibly in clinical rehabilitation of

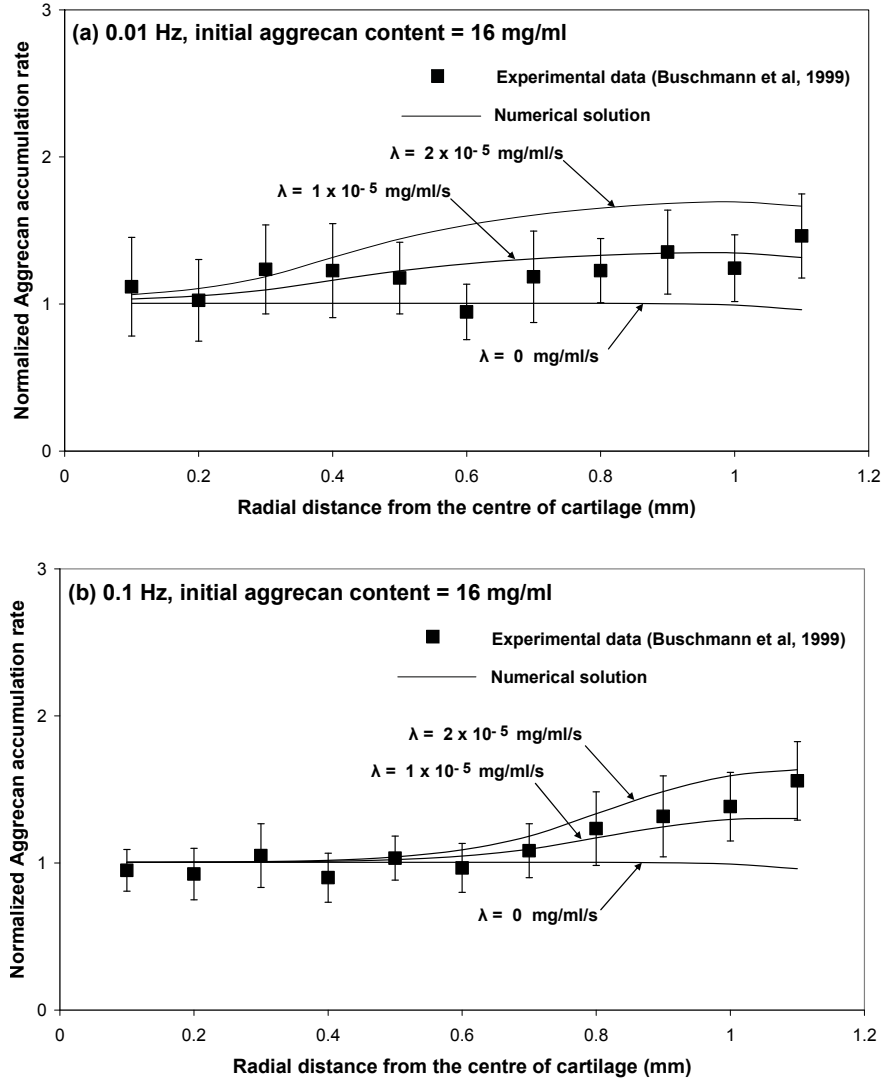


Figure 3: Fitting of the numerical predictions to the experimental data from Buschmann et al [13]. Spatially dependent synthetic rate of aggrecan in dynamically compressed cartilage disk is normalized to the control mean. (a) 0.01 Hz, (b) 0.1 Hz.

joints.

The parameters in the numerical model may be adjusted to fit the measured aggrecan synthesis data from Bonassar et al [21] and Jin et al [22] when cartilage explants were exposed to a range of IGF-I concentrations. As the concentration of free, bound and degraded aggrecan is generally non-uniform in the radial direction, it is useful to define the normalized average concentration of each aggrecan component using the following

equations: Free aggrecan:

$$\bar{c}_{avg}^f = \frac{1}{\bar{c}_{a0}} \left( \frac{\int_0^{r_0} 2\pi r \bar{c}_a^f dr}{\int_0^{r_0} 2\pi r dr} \right) \quad (4.1a)$$

Bound aggrecan:

$$\bar{c}_{avg}^b = \frac{1}{\bar{c}_{a0}} \left( \frac{\int_0^{r_0} 2\pi r \bar{c}_a^b dr}{\int_0^{r_0} 2\pi r dr} \right) \quad (4.1b)$$

Degraded aggrecan:

$$\bar{c}_{avg}^d = \frac{1}{\bar{c}_{a0}} \left( \frac{\int_0^{r_0} 2\pi r \bar{c}_a^d dr}{\int_0^{r_0} 2\pi r dr} \right) \quad (4.1c)$$

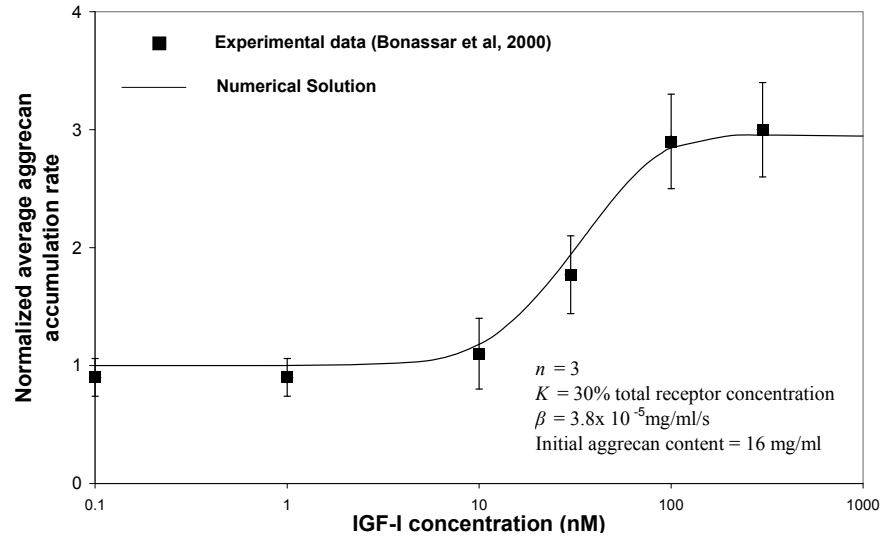


Figure 4: Fitting of the numerical predictions to the IGF-I dose-response experimental studies from Bonassar et al [21].

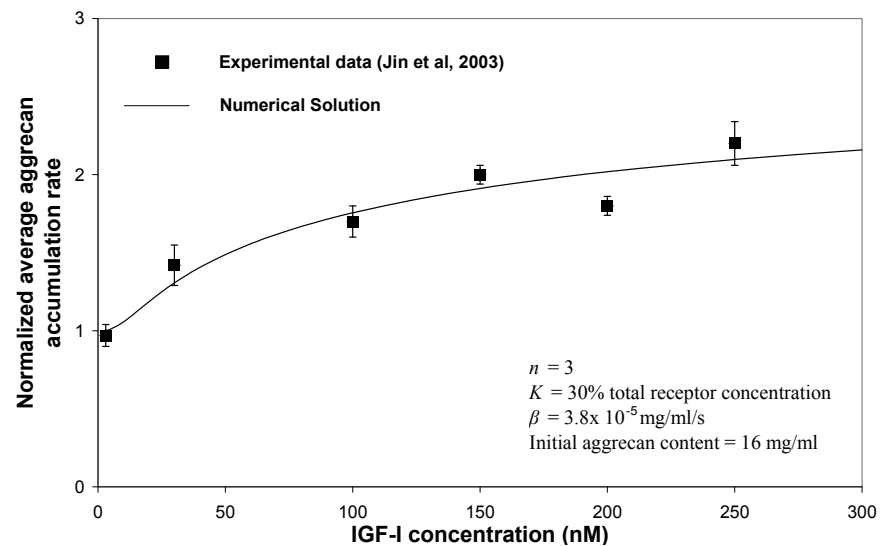


Figure 5: Fitting of the numerical predictions to the IGF-I dose-response experimental studies from Jin et al [22].

Remarkably, with suitable parameter choice the numerical model is able reproduce the trends in the measured biosynthesis data from both experiments. The parameters employed in the model were taken to be  $\bar{c}_{a0} \approx 16$  mg/ml,  $n \approx 3$ ,  $K \approx 30\%$  total receptor concentration, and  $\beta \approx 3.8 \times 10^{-5}$  mg/ml·s (Figure 4 and Figure 5). The estimate of  $\bar{c}_{a0}$  is consistent with previous experimental studies showing the aggrecan content of bovine cartilage ranges from 10 – 50 mg/ml [30, 31]. Furthermore, Figure 4 shows that there is a threshold of

IGF-I concentration (at around 10 nM), at which a significant increase of aggrecan production is triggered, but the effects of IGF-I on biosynthesis reaches a plateau when IGF-I concentration  $> 100$  ng/ml.

While this model parameters estimation based on available data is very encouraging, given the limited experimental information to date, the model clearly needs to be further validated against future experimental datasets, including studies consider-

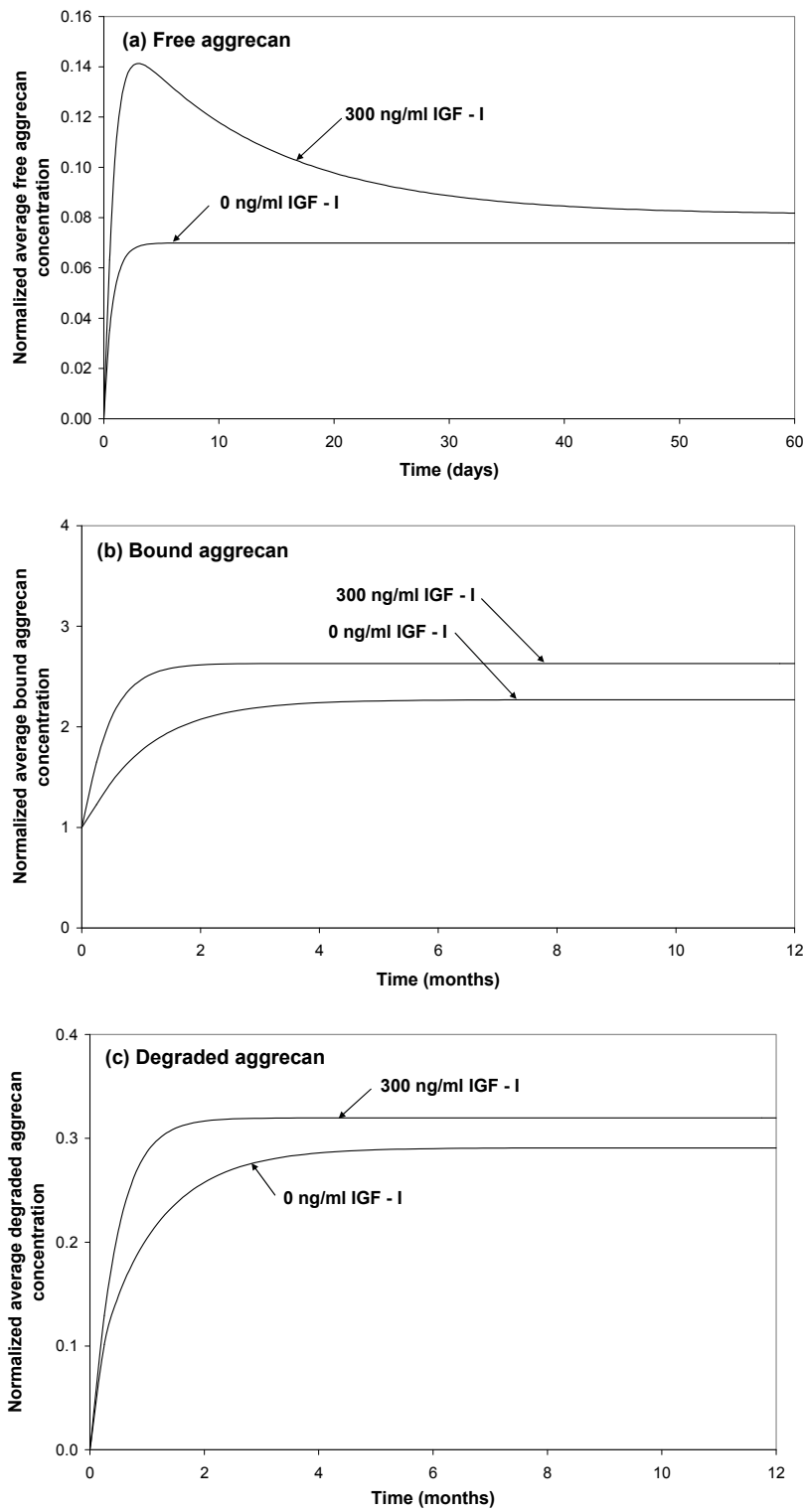


Figure 6: Effect of IGF-I on time dependent free, bound and degraded aggrecan concentration profiles under free diffusion. (a) Free aggrecan; (b) Bound aggrecan; (c) Degraded aggrecan.

ing the combined effect of IGF-I and mechanical loading. Nevertheless, the model proposed here provides a useful start in modeling aggrecan production and removal, and allows quantitative predictions to be made and explored. The following sections detail some predictions made by the model.

## 5 Theoretical prediction of aggrecan synthesis in cartilage

### 5.1 Free diffusion

The validated computational model is now employed to predict the time dependent aggrecan concentration, with or without the treatment of 300 ng/ml IGF-I. It can be seen from Figure 6 that IGF-I increases steady-state free aggrecan by 17%, bound aggrecan by 16% and degraded aggrecan by 10% in comparison to the basal condition (no treatment of IGF-I). In addition, in the absence of IGF-I, free aggrecan concentration reaches its steady-state at around 5 days (Figure 6a), whereas bound and degraded aggrecan concentrations take much longer time to reach their steady-state (around 11 months) (Figure 6b-c). However, when the influence of 300 ng/ml IGF-I is included, it is observed that free aggrecan concentration increases very significantly at early time, reaching its peak at around 2~3 days, and then gradually decreases to its steady-state at around 2 months (Figure 6a). One explanation for these findings is that it takes a relatively short time for the IGF-I to diffuse into cartilage tissue, with its stimulation effect on biosynthesis reaching its maximal level when IGF-I fully saturates the cartilage disk on a timescale of days. The increase in free aggrecan then stimulates proteoglycan on a longer timescale, the increased proteoglycan concentration leads to increased degradation. IGF-I was seen to reduce the time for bound and degraded aggrecan to reach their equilibrium (Figure 6b-c). Although it would be very difficult to test a hypothesis based on the need for such long term culture experiments to test and compare to the predictions of Figure 6, it is interesting and potentially important to note the wide range of time scales that can result from the combination

of loading and growth factor stimulation, and the fact that certain pathways may, indeed, involve longer duration processes than others.

### 5.2 Free diffusion with cyclic deformation

Chondrocytes can sense various signals ranging from biochemical information transmitted by growth factors and cytokines to physical stimuli (like matrix deformation and interstitial fluid flow). Throughout life, chondrocytes respond to these signals by producing appropriate matrix proteins that assemble in the extracellular environment to maintain the normal function of tissue in order to withstand external mechanical forces. Figure 7 investigates the individual as well as the combined effect of IGF-I and mechanical stimulation on time dependent synthesis of aggrecan within the cartilage. It can be seen from Figure 7a that IGF-I alone at 300 ng/ml stimulates free aggrecan synthesis by around 100% in comparison to basal condition (i.e. 0 ng/ml IGF-I, no loading), mechanical loading alone at 0.01 Hz and 10% strain amplitude increases free aggrecan concentration by around 20%, but when applied together, the degree of aggrecan stimulation is greater than that achieved by either IGF-I or mechanical loading alone (at around 120%). Figure 7b shows the effects of IGF-I and mechanical loading on bound aggrecan concentration. During the first 20 hours, IGF-I, mechanical loading and the combination of the two stimuli lead to a slight increase of bound aggrecan concentration at around 2.3%, 0.7% and 3.0% compared to the basal condition respectively. The implication of this numerical outcome is that during a short time scale (e.g., 20 hours), only a small fraction of newly synthesized aggrecan molecules are able to effectively be immobilized within the ECM because the actual accumulation process normally take much longer time (e.g. in months as shown in Figure 6b). As for the degraded aggrecan, its concentration shows little difference in the presence of either IGF-I or mechanical loading due to the relative stability of bound aggrecan and the short time scale considered here (Figure 7c).

In order to understand the spatial biosynthesis behavior under IGF-I and mechanical loading, the

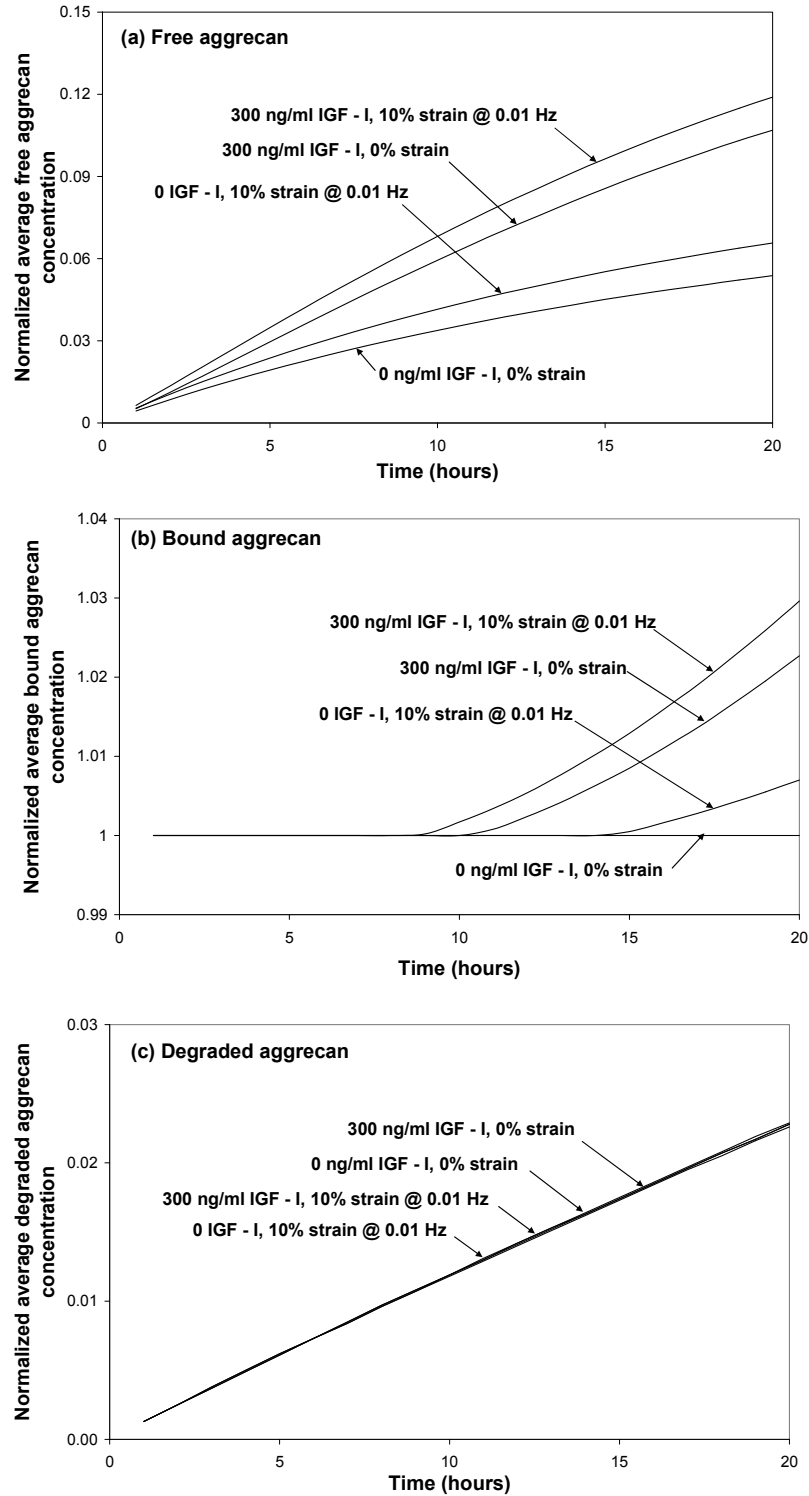


Figure 7: Effect of IGF-I and mechanical stimuli on time dependent free, bound and degraded aggrecan concentration profiles. (a) Free aggrecan; (b) Bound aggrecan; (c) Degraded aggrecan.

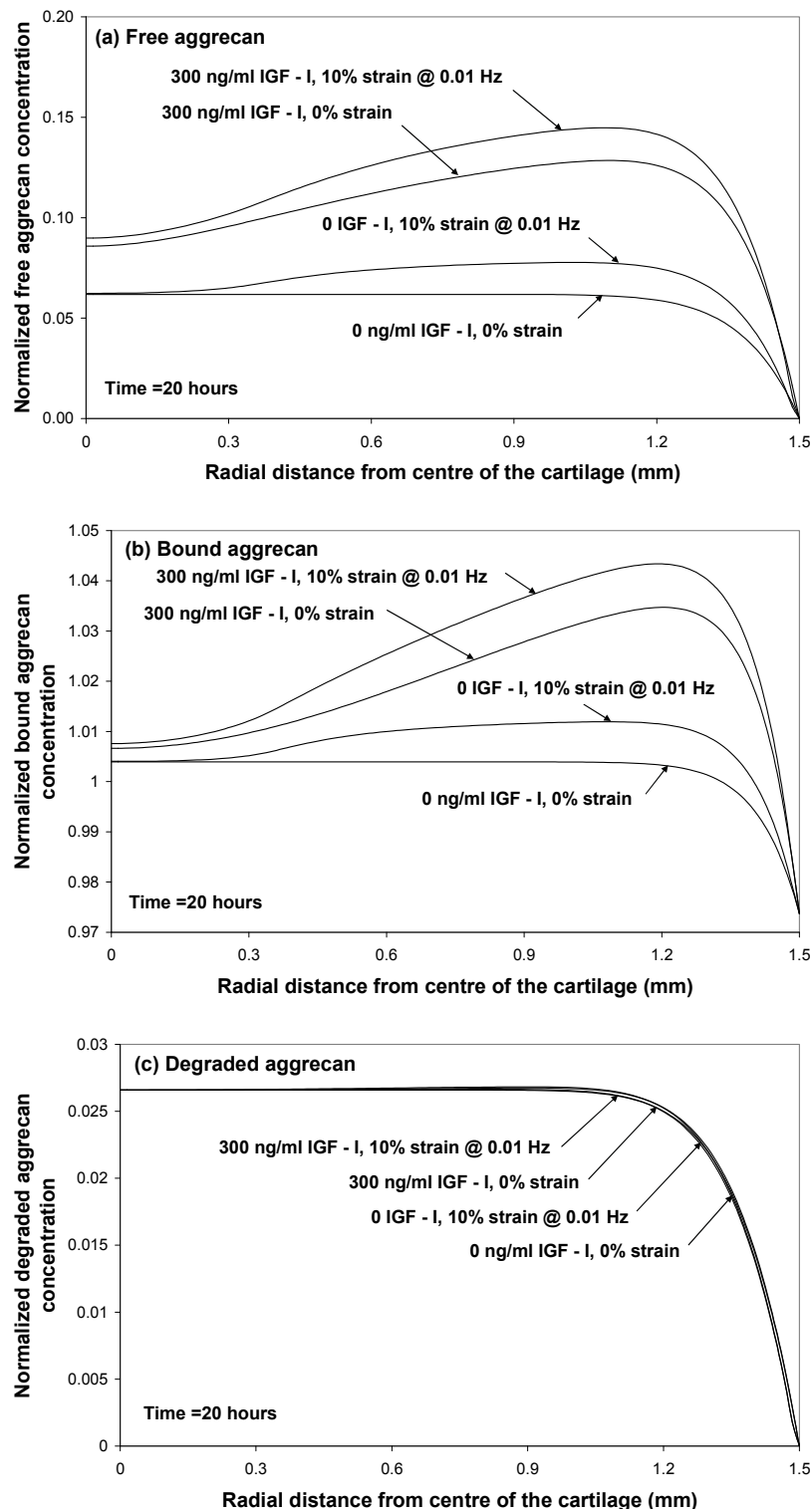


Figure 8: Effect of IGF-I and mechanical stimuli on spatially dependent free, bound and degraded aggrecan concentration profiles. The numerical predictions are normalized to initial total aggrecan concentration ( $\bar{c}_{d0} = 16$  mg/ml). (a) Free aggrecan; (b) Bound aggrecan; (c) Degraded aggrecan.

model was employed to estimate the spatial aggrecan concentration profiles, which are not easily observed experimentally. The cartilage is subjected to 300 mg/ml IGF-I, 0.01 Hz @ 10% strain for 20 hours, and the corresponding results are shown in Figure 8. It can be observed from Figure 8a-b that in comparison to mechanical stimulation, IGF-I induced biosynthesis is more obvious and seen throughout the entire cartilage disk, although the greatest stimulation was seen near the periphery where there is a relatively higher IGF-I concentration. Again for the degraded aggrecan, there is little observed effect during the first 20 hours.

### 5.3 Parametric study

Due to limited experimental information on likely tortuosities of the ECM relating to diffusion, and hinderance by the ECM relating to advective transport, a parametric study was carried out to investigate the relationships between the cartilage biosynthesis behavior, matrix distribution and matrix aggrecan transport coefficients. Figure 9a compares IGF-I mediated biosynthesis with  $K_d = 0.1$  or  $1.0$ . Results show that  $K_d = 0.1$  reduces free aggrecan diffusion into the centre of the cartilage from the periphery, and leads to a significant increase of free aggrecan concentration at the periphery. When hindered transport of free aggrecan was considered, a similar phenomenon was also observed (in Figure 9b-c). The results indicate in both cases that reduced transport, either by reduced diffusion or reduced effectiveness of advective transport, leaves the aggrecan macromolecules close to where they were produced.

The aim of tissue engineering research is to develop a viable replacement for damaged tissue. Optimal selection of initial cell density is essential for the successful in vitro cultivation of large tissue constructs [32]. Figure 10 predicts the spatially dependent normalized free aggrecan concentration at total chondrocyte receptor concentrations 0.6 nM and 6nM respectively after 15 hour treatment of IGF-I (300 ng/ml) in combination of dynamic compression (10% strain @ 0.01 Hz). It can be seen that at early times (e.g., the first 5 hours), there is little difference in

the spatially dependent aggrecan production between these two concentrations (i.e., 0.6 nM and 6 nM). However, with increased time, much greater biosynthesis is seen in the interior region of cartilage at low receptor concentration (i.e., 0.6 nM) compared to that at high receptor concentration (i.e., 6 nM). This observation may be explained by the likelihood that most of the IGF-I binds to cell receptors at the periphery of the cartilage disks when receptor concentration is high, so at low concentrations of IGF-I and high receptor density, there is little chance that IGF-I will reach the interior of the tissue. We envisage that this approach may be useful in identifying optimal cell density distributions for efficient protein synthesis and more uniform cartilage development in tissue engineered constructs.

## 6 Conclusion

In this paper, we developed a quantitative model to describe the coupled processes of growth factor and matrix molecule transport, interstitial flow (induced by the mechanical deformation of the cartilage), to better understand homeostasis within cartilage. The model builds on our previous publications by incorporating proteoglycan biosynthesis and degradation in the model. The proposed model was validated using a series of experimental data. The greatest parameter uncertainties in the model were those relating to aggrecan biosynthesis. However there are three independent studies on aggrecan-GAG production performed on 1-2 week old bovine calf cartilage explants that were the basis of our model development [13, 21, 22]. A key challenge was to find a single set of parameters that are consistent with the aggrecan biosynthesis behavior observed in all three independent experimental studies [13, 21, 22]. Parameters in Equations (2.9) and (2.10) that needed to be estimated include the coefficient  $n$ , the activation coefficient  $K$ , the IGF-I mediated maximum production rate  $\beta$ , and mechanical stimuli mediated production rate  $\lambda$ , as well as estimating the initial aggrecan concentration  $\bar{c}_{g0}$ . A major outcome of this paper was identifying a single consistent set of parameters for aggrecan production in juvenile bovine cartilage subject to

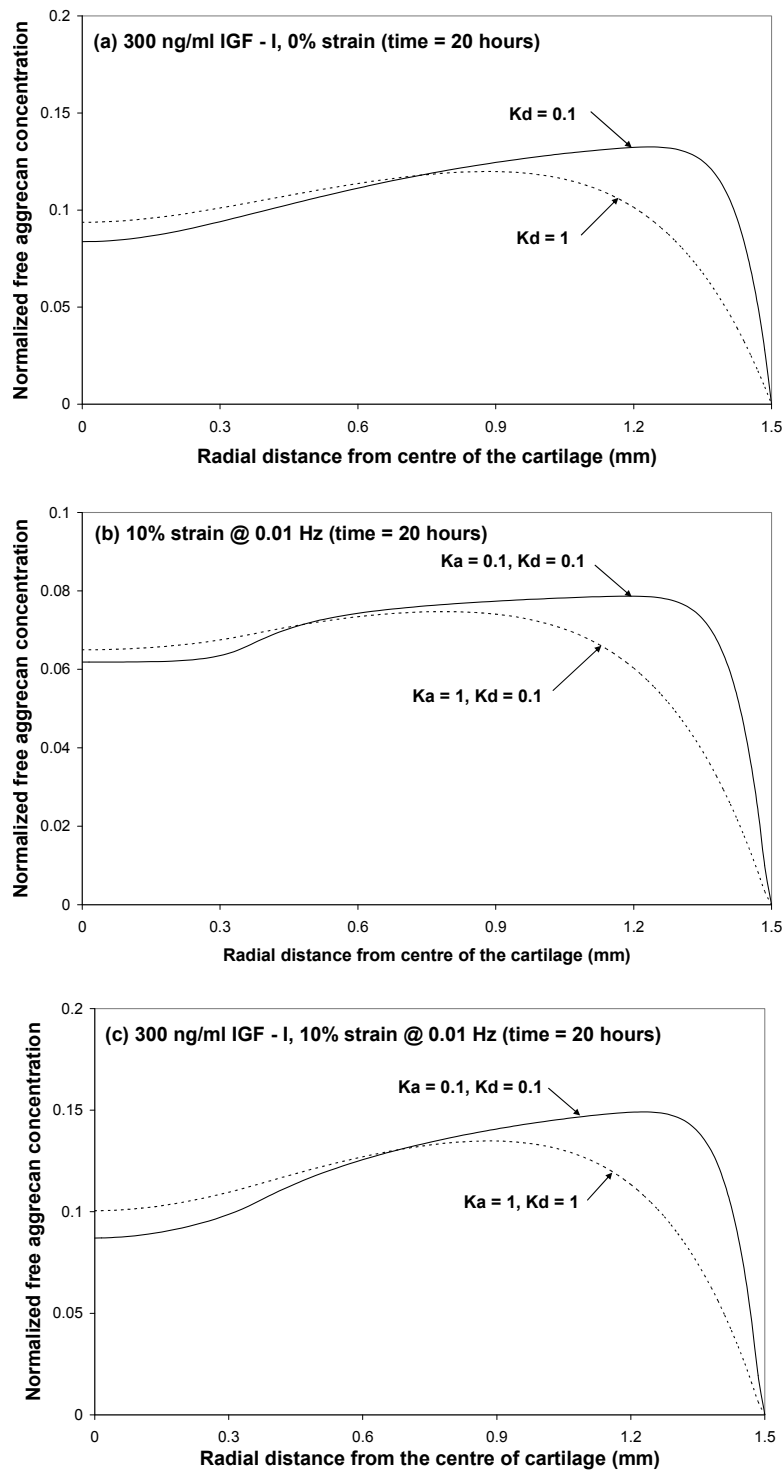


Figure 9: Comparison of free aggrecan concentration as a function of radial distance from centre of the cartilage under various dimensionless tortuosity and hindrance coefficients. The numerical predictions are normalized to initial total aggrecan concentration ( $\bar{c}_{a0} = 16$  mg/ml). (a) Free diffusion of 300 ng/ml IGF-I; (b) Dynamic compression at 10% strain @ 0.01 Hz; (c) The combination of IGF-I and dynamic compression.

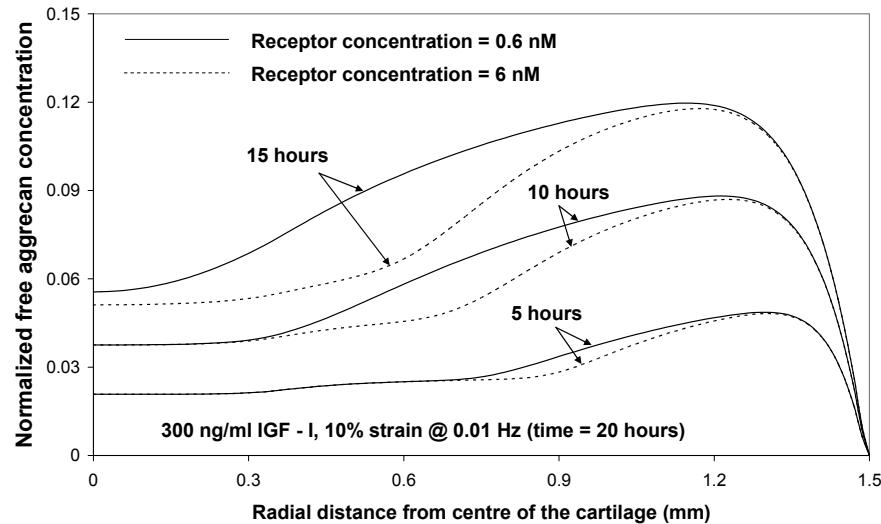


Figure 10: Comparison of free aggrecan concentration as a function of radial distance from centre of the cartilage at various total receptor concentrations. The numerical predictions are normalized to initial total aggrecan concentration ( $\bar{c}_{a0} = 16$  mg/ml).

chemical and mechanical stimulation.

Based on the model, quantitative predictions were made as to how cartilage would respond to chemical and mechanical stimulation. While further validation of the model against future experimental datasets (e.g. involving humans) is obviously necessary, the model proposed nevertheless provides a useful starting point for understanding cartilage homeostasis, and may be useful in explaining the behaviour of tissue constructs and ultimately disease and repair processes.

**Acknowledgement:** The authors wish to thank The Australian Research Council (DP50192), The University of Melbourne, and NIH Grant AR33236 for their support.

## References

1. J. Dudhia, (2005) Aggrecan, aging and assembly in articular cartilage, *Cellular and Molecular Life Sciences* 62 2241-2256.
2. N.O. Chahine, F.H. Chen, C.T. Hung, G.A. Ateshian, (2005) Direct Measurement of Osmotic Pressure of Glycosaminoglycan Solutions by Membrane Osmometry at Room Temperature, *Biophysical Journal* 89 1543–1550.
3. S. Bolis, C.J. Handley, W.D. Comper, (1989) Passive loss of proteoglycan from articular cartilage explants, *Biochem. Biophys. Acta* 993 157-167.
4. J.D. Sandy, J.R. O’Neill, L.C. Ratzlaff, (1989) Acquisition of hyaluronate-binding affinity in vivo by newly synthesized cartilage proteoglycans, *Biochemical Journal* 258 875-880.
5. L.A. Pottenger, J.E. Webb, N.B. Lyon, (1985) Kinetics of extraction of proteoglycans from human cartilage, *Arthritis & Rheumatism* 28 323-330.
6. M.A. DiMicco, R.L. Sah, (2003) Dependence of cartilage matrix composition on biosynthesis, diffusion and reaction, *Transport in Porous Media* 50 57-73.
7. T.J. Klein, R.L. Sah, (2007) Modulation of depth-dependent properties in tissue-engineered cartilage with a semi-permeable membrane and perfusion: a continuum model of matrix metabolism and transport, *Biomechanics and Modeling in Mechanobiology* 6 21-23.
8. R.L. Mauck, C.T. Hung, G.A. Ateshian, (2000) Modeling of neutral solute transport in

- a dynamically loaded porous permeable gel: implications for articular cartilage biosynthesis and tissue engineering, *Journal of Biomechanical Engineering* 125 602-614.
9. L. Zhang, A.Z. Szeri, (2005) Transport of neutral solute in articular cartilage: effects of loading and particle size, *Proceedings of the Royal Society* 461 2021-2042.
  10. F.P. Luyten, V.C. Hascall, S.P. Nissley, T.I. Morales, A.H. Reddi.,(1988) Insulin-like growth factors maintain steady-state metabolism of proteoglycans in bovine articular cartilage explants, *Archives of Biochemistry and Biophysics* 267 416-425.
  11. A.J. Grodzinsky, M.E. Levenston, M. Jin, E.H. Frank, (2000) Cartilage Tissue Remodeling In Response To Mechanical Forces, *Annual Review of Biomedical Engineering* 2 691-713.
  12. E.M. Roos, L. Dahlberg, (2005) Positive effects of moderate exercise on glycosaminoglycan content in knee cartilage: A four-month, randomized, controlled trial in patients at risk of osteoarthritis, *Arthritis & Rheumatism* 52 3507-3514.
  13. M.D. Buschmann, Y.-J. Kim, M. Wong, E. Frank, E.B. Hunziker, A.J. Rodzinsky, (1999) Stimulation of aggrecan synthesis in cartilage explants by cyclic loading is localized to regions of high interstitial fluid flow, *Archives of Biochemistry and Biophysics* 366 1-7.
  14. T. Davisson, S. Kunig, A. Chen, R. Sah, A. Ratcliffe, (2002) Static and dynamic compression modulate matrix metabolism in tissue engineered cartilage, *Journal of Orthopaedic Research* 20.
  15. B.P. O'Hara, J.P.G. Urban, A. Maroudas, (1990) Influence of cyclic loading on the nutrition of articular cartilage, *Annals of Rheumatic Diseases* 49 536-539.
  16. L. Zhang, B.S. Gardiner, D.W. Smith, P. Pivonka, A.J. Grodzinsky, (2007) The effect of cyclic deformation and solute binding on solute transport in cartilage, *Archives of Biochemistry and Biophysics* 457 47-56.
  17. W.D. Comper, R. Williams, (1987) Hydrodynamics of concentrated proteoglycan solutions, *Journal of Biological Chemistry* 262 13464-13471.
  18. B.S. Gardiner, D.W. Smith, P. Pivonka, A.J. Grodzinsky, E.H. Frank, L. Zhang, (2007) Solute transport in cartilage undergoing cyclic deformation, *Computer Methods in Biomechanics and Biomedical Engineering* 10 265-278.
  19. L. Zhang, B.S. Gardiner, D.W. Smith, P. Pivonka, A.J. Grodzinsky, (2007) IGF uptake with competitive binding in articular cartilage, *Journal of Biological Systems* Accepted.
  20. L. Zhang, B.S. Gardiner, D.W. Smith, P. Pivonka, A.J. Grodzinsky, (2007) An integrated model of IGF-I mediated biosynthesis in deforming articular cartilage. *Journal of Engineering Mechanics (ASCE)* Accepted.
  21. L.J. Bonassar, A.J. Grodzinsky, A. Srinivasan, S.G. Davila, S.B. Trippel, (2000) Mechanical and physiochemical regulation of the action of insulin-like growth factor-i on articular cartilage, *Archives of Biochemistry and Biophysics* 379 57-63.
  22. M. Jin, G.R. Emkey, P. Siparsky, S.B. Trippel, A.J. Grodzinsky,(2003) Combined effects of dynamic tissue shear deformation and insulin-like growth factor I on chondrocyte biosynthesis in cartilage explants, *Archives of Biochemistry and Biophysics* 414 223-231.
  23. D.S. Schalch, C.M. Sessions, A.C. Farley, A. Masakawa, C.A. Emler, D.G. Dills, (1986) Interaction of insulin-like growth factor I/somatomedin-C with cultured rat chondrocytes: receptor binding and internalization, *Endocrinology* 118 1590-1597.
  24. U. Alon, (2006) An introduction to systems biology, Chapman & Hall/CRC, *Taylor & Francis Group*.

25. C.G. Wilson, L.J. Bonassar, S.S. Kohles, (2002) Modeling the dynamic composition of engineered cartilage, *Archives of Biochemistry and Biophysics* 408 246-254.
26. B. Obradovic, J.H. Meldon, L.E. Freed, G. Vunjak-Novakovic, (2000) Glycosaminoglycan deposition in engineered cartilage: Experiments and mathematical model, *AIChE Journal* 46 1860-1871.
27. M.A. Soltz, G.A. Ateshian, (2000) A Conewise Linear Elasticity Mixture Model for the Analysis of Tension-Compression Non-linearity in Articular Cartilage, *Journal of Biomechanical Engineering* 122 576-586.
28. FEMLAB, (2003) COMSOL, Inc., MA, USA.
29. A. Edwards, W.M. Deen, B.S. Daniels, (1997) Hindered transport of macromolecules in isolated glomeruli. I. Diffusion across intact and cell-free capillaries, *Biophysical Journal* 72 204-213.
30. M.R. Disilvestro, J.-K.F. Suh, (2002) Biphasic Poroviscoelastic Characteristics of Proteoglycan-Depleted Articular Cartilage: Simulation of Degeneration, *Annals of Biomedical Engineering* 30.
31. V.C. Mow, A.F. Mak, W.M. Lai, L.C. Rosenberg, L.-H. Tang, (1984) Viscoelastic properties of proteoglycan subunits and aggregates in varying solution concentrations, *Journal of Biomechanics* 17 325-338.
32. G. Vunjak-Novakovic, B. Obradovic, I. Martin, P.M. Bursac, R. Langer, L.E. Freed, (1998) Dynamic Cell Seeding of Polymer Scaffolds for Cartilage Tissue Engineering, *Biotechnology Progress* 14 193-202.
33. V.C. Mow, J.S. Hou, J.M. Owens, A. Ratcliffe, (1990) Biphasic and quasilinear viscoelastic theories for hydrated soft tissues, *Biomechanics of Diarthrodial Joints*, Springer-Verlag, New York 215-260.
34. N.R. Bhakta, A.M. Garcia, E.H. Frank, A.J. Grodzinsky, T.I. Morales, (2000) The Insulin-like Growth Factors (IGFs) I and II Bind to Articular Cartilage via the IGF-binding Proteins, *The Journal of Biological Chemistry* 275 5860-5866.
35. T.I. Morales, (1997) The Role and Content of Endogenous Insulin-Like Growth Factor-Binding Proteins in Bovine Articular Cartilage, *Archives of Biochemistry and Biophysics* 343 164-172.
36. E. Barta, A. Maroudas, (2006) A theoretical study of the distribution of insulin-like growth factor in human articular cartilage, *Journal of Theoretical Biology* 241 628-638.

